*29th EPS Conference on Plasma Phys. and Contr. Fusion Montreux, 17-21 June 2002 ECA Vol. **26B**, P-4.089 (2002)*

Radial Electric Field in the Biasing Experiments and Effective Conductivity in a Tokamak

V. Rozhansky[*], E. Kaveeva[*], S. Voskoboynikov[*], D. Coster[**], X. Bonnin [***], R. Schneider[***]

[*] *St.Petersburg State Technical University, 195251 St.Petersburg, Russia*
[**] *Max-Planck Institut für Plasmaphysik, EURATOM Association, D-85748 Garching, Germany*
[***] *Max-Planck Institut für Plasmaphysik, EURATOM Association, D-17491 Greifswald, Germany*

I. Introduction

On several tokamaks (CCT, TUMAN-3, TEXTOR and others) the biasing experiments were performed. The potential of few hundred eV was applied to the core flux surface with respect to the limiter. The measured I-V characteristics and profiles of electric field should be explained thus providing understanding of the effective perpendicular conductivity and of the mechanisms responsible for the formation of the radial electric field. In the existing models (see [1] and references therein) the radial current was calculated using the toroidal and parallel projections of the momentum balance equation. The $\vec{j}\times\vec{B}$ force accelerates plasma toroidally and is balanced by the force associated with the radial transport of the toroidal velocity due to anomalous diffusion and anomalous perpendicular viscosity. Since in the parallel momentum balance equation this force is balanced mainly by the averaged parallel viscosity, the radial current may be expressed through the parallel viscosity. Using the dependence of the parallel viscosity on the radial electric field, the radial current as a function of the electric field has been calculated. In a similar approach [2], it was assumed that the $\vec{j}\times\vec{B}$ force is balanced by the ion-neutral friction. The models, where the radial current is proportional to the parallel viscosity, are consistent with the value of the plasma resistance for small voltages. In the experiments at large voltages the current started to decrease. This was associated with the decrease of the parallel viscosity when the poloidal drift velocity reaches the poloidal sound speed $b_x c_s$. Recently the biasing experiments were simulated by Monte-Carlo code [3]. The solitary structures were observed for large voltages but the anomalous terms were absent and, therefore, it is difficult to judge on their role.

Below the biasing experiments and the problem of the effective perpendicular conductivity are studied on the basis of the Braginski equations, where the perpendicular transport coefficients are replaced by their anomalous values. The simulations were performed by B2SOLPS5.0 code [4] in the real divertor geometry. Three regimes exist, which correspond to the different values of the effective perpendicular conductivity and to

different profiles of the electric field. The key parameter κ depends on the magnetic pumping frequency and anomalous diffusion coefficient.

2. Analytical model for the perpendicular current

We combine equations of parallel and toroidal momentum balance (y is the radial, x is the poloidal coordinate, I is the net current, S is the flux surface area)

$$\left\langle\left\langle j_y \right\rangle\right\rangle = \frac{I}{S} = -<<\frac{\vec{B}\cdot(\nabla\cdot\vec{\pi}_\perp + nm_i\frac{d\vec{V}}{dt})}{BB_x}>>=\frac{<\vec{B}\cdot\nabla\cdot\vec{\pi}_\parallel>}{<BB_x>}+\delta, \qquad (1)$$

$$\delta = \frac{<\vec{B}\cdot(\nabla\cdot\vec{\pi}_\perp + nm_i\frac{d\vec{V}}{dt})\cdot(1-\frac{<<B^2>>}{B^2})>}{<BB_x>}. \qquad (2)$$

We neglect the friction with neutrals with respect to the terms responsible for the radial transport of the toroidal (parallel) momentum. We introduce

$$\kappa = \frac{\nu^{(mp)}L_y^2}{D} \quad , \qquad (3)$$

where $\nu^{(mp)}$ is the magnetic pumping frequency, D is the anomalous diffusion coefficient, L_y is the distance between the electrode and the separatrix. The solution of Eq. (1) depends on κ, for further details see [5]. For $1>\kappa>\varepsilon^2$, $\varepsilon = r/R$

$$\left\langle\left\langle j_y \right\rangle\right\rangle = -\nu^{(mp)}nm_i\frac{B}{\langle BB_x\rangle B_x h_y}\left[\frac{\partial\varphi}{\partial y}+\frac{T_i}{e}\left(\frac{\partial\ln n}{\partial y}+k_T\frac{\partial\ln T_i}{\partial y}\right)\right] \qquad (4)$$

for small applied voltages in accordance with [1]. However, for $\kappa>1$ the solution is quite different. In this regime the contribution of the toroidal rotation term to the parallel viscosity is quite significant, the poloidal rotation is small with respect to the contributions from the toroidal rotation and $\vec{E}\times\vec{B}$ drifts: $V_x << \frac{B_x}{B}V_z$; $V_x \sim \kappa^{-1}\frac{B_x}{B}V_z$; $\frac{E_y}{B} \cong -\frac{B_x}{B}V_z$. The radial electric field is hence given by the neoclassical expression $E_y^{(NEO)} = \frac{T_i}{e}(\frac{1}{h_y}\frac{d\ln n}{dy}+k_T\frac{1}{h_y}\frac{d\ln T_i}{dy})-\frac{B_x}{B}\langle BV_z\rangle$. The current is

$$\left\langle\left\langle j_y \right\rangle\right\rangle = \left\langle\left\langle \frac{1}{h_z B_x\sqrt{g}}\frac{\partial}{\partial y}\left\{\frac{h_z\sqrt{g}}{h_y}(m_i\Gamma_y - \frac{\eta_2}{h_y}\frac{\partial}{\partial y})\left[\frac{E_y}{B_x}-\frac{T_i}{B_x e}\left(\frac{1}{h_y}\frac{d\ln n}{dy}+\frac{k_T}{h_y}\frac{d\ln T_i}{dy}\right)\right]\right\}\right\rangle\right\rangle, \qquad (5)$$

where $\Gamma_y = -D\frac{\partial n}{h_y \partial y}$ is a particle flux, $\eta_2 = nm_iD$. The case $\kappa < \varepsilon^2$ is more complicated [5].

3. Modeling

The simulations were performed for the edge plasma of the ASDEX-Upgrade. The biasing potential was imposed at the inner boundary of the grid. The ion-neutral friction in the toroidal (parallel) momentum balance equation was much smaller than the terms responsible for the radial transport of the toroidal (parallel) momentum, Fig.1. For the modeling of the regime $\kappa > 1$ were chosen: $n\,|_{r-r_s=-1cm} = 0.5 \cdot 10^{19} m^{-3}$, $P = 80KW$. Poloidal velocity versus current is shown in Fig.2. The poloidal $\vec{E} \times \vec{B}$ drift here compensates the contribution from the toroidal velocity. The radial electric field profile is compared with the analytical predictions in Fig.3. The dashed line 2 corresponds to the zero boundary condition for the toroidal rotation and hence to the zero radial electric field at the separatrix, the dashed line 3 corresponds to the boundary condition taken from the code. The electric field is consistent with Eq. (5). The I-V characteristic is shown in Fig. 4. It is almost linear at medium voltages with the slope close to that predicted by analytical expressions. For higher voltages the nonlinear effects are significant since V_z approaches the sound speed. For $1 > \kappa > \varepsilon^2$ were chosen: $n|_{r-r_s=-1cm} = 2.7 \cdot 10^{19} m^{-3}$, $P = 0.4\,MW$, $\kappa \approx 0.1$. Poloidal velocity is shown in Fig.5. For the small voltages the poloidal rotation is of the order of the poloidal $\vec{E} \times \vec{B}$ drift, the toroidal rotation contribution is smaller then the poloidal $\vec{E} \times \vec{B}$ drift. The radial electric field in this regime is proportional to the current Eq. (4). Calculated and analytical electric fields are shown in Fig.6. The I-V characteristic is shown in Fig.7. The results for medium voltages are in agreement with theoretical predictions. There is no saturation at high voltages due to the peculiarities of the Pfirsch-Schlueter regime. Regime $\kappa < \varepsilon^2$ is not discussed here.

References

1. V. Rozhansky and M. Tendler, in Reviews of Plasma Phys. Ed. by B.B. Kadomtsev, Consultants Bureau N.Y.-London **19,** 147 (1996).
2. R. R. Weynants, G. Vanoost, G. Bertschinger *et al*., Nuclear Fusion **32,** 837 (1992).
3. J. Heikkinen, S. Jachmich, T.P. Kiviniemi, T. Kurki-Suonio, A.G. Peeters, Phys. Plasmas **8,** 2824 (2001).
4. V. Rozhansky, S. Voskoboynikov, E. Kaveeva, D. Coster, R. Schneider, Nucl. Fus. **41,** 387 (2001).
5. V. Rozhansky, S. Voskoboynikov, E. Kaveeva, D. Coster, X. Bonnin, R. Schneider, Phys. Plasmas **9** (2002) (accepted).

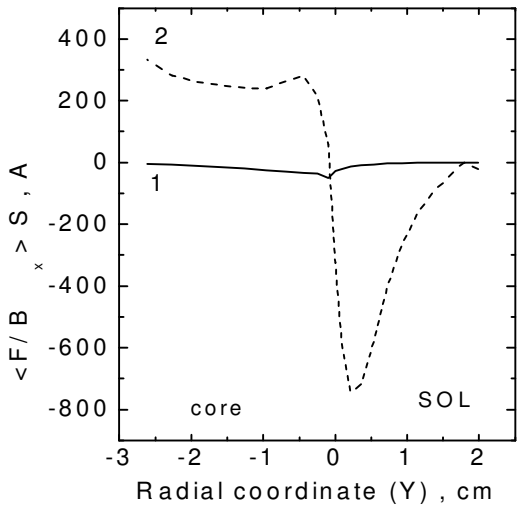

Fig.1. Toroidal components of the averaged momentum balance for discharge parameters $\varphi|_{electrode} = 1000\ V$, $n|_{-1cm} = 2 \cdot 10^{19}\ m^{-3}$, $T_i|_{-1cm} = 40eV$: 1- ion-neutral friction force; 2- divergence of the radial flux of toroidal momentum.

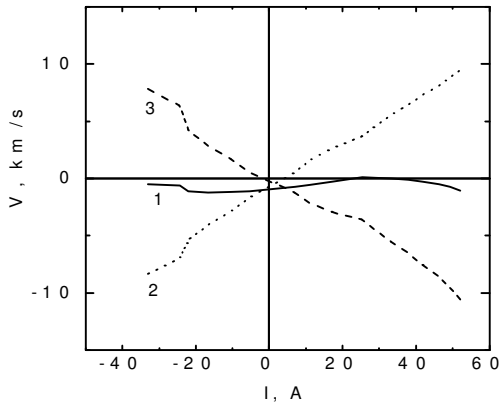

Fig.2. Dependencies of the different components of averaged poloidal velocity on the net current for $\kappa > 1$: 1- net poloidal velocity; 2- $\vec{E} \times \vec{B}$ velocity; 3- poloidal projection of the parallel velocity.

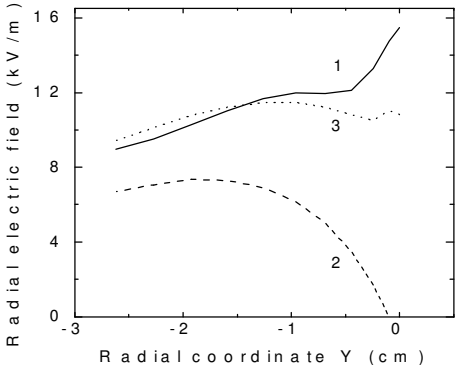

Fig.3. Radial electric field profile for $\kappa > 1$: 1- calculated profile; 2- theoretical prediction for $V_{\|} = 0$ at the separatrix; 3- theoretical profile for the code boundary condition.

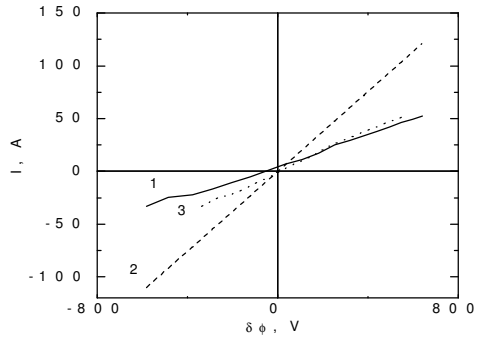

Fig.4. I-V characteristic for $\kappa > 1$: 1-calculated characteristic; 2-theoretical prediction for $V_{\|} = 0$ at the separatrix; 3-theoretical characteristic for the code boundary condition.

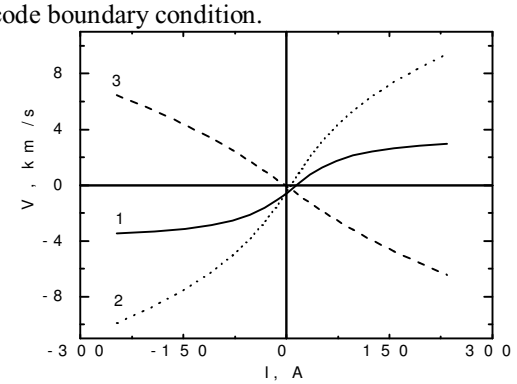

Fig.5. Dependencies of the different components of average poloidal velocity on the net current for $\kappa < 1$: 1- net poloidal velocity; 2- $\vec{E} \times \vec{B}$ velocity; 3-poloidal projection of the parallel velocity.

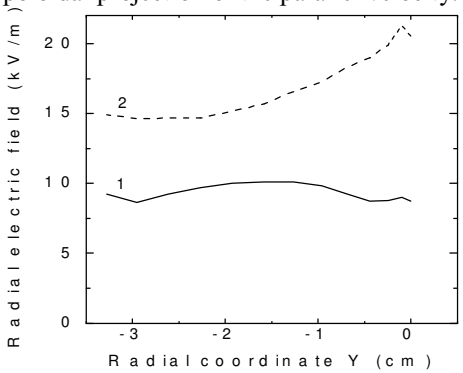

Fig.6. Radial electric field profile for $\kappa < 1$: 1-calculated profile; 2-theoretical prediction.

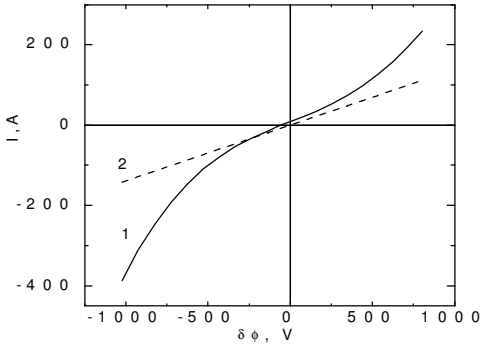

Fig.7. I-V characteristic for $\kappa < 1$: 1-calculated characteristic; 2-theoretical prediction.